Progress In Electromagnetics Research C, Vol. 42, 55–66, 2013

INDEPENDENTLY-TUNED DUAL-BAND FILTER USING VARACTOR-LOADED RESONATORS

Xiu Yin Zhang[1], Li Gao[1, *], Yunfei Cao[2], Xiao-Lan Zhao[1], and Yong Ding[3]

[1]School of Electronic and Information Engineering, South China University of Technology, Guangzhou 510640, China

[2]Department of Electrical and Electronic Engineering, The University of Hong Kong, Hong Kong, China

[3]Tongyu Communication Inc., Zhoushan 528437, China

Abstract—This paper presents a high-selectivity dual-band bandpass filter with independently-tunable passband frequencies. A tap-coupled structure is utilized to feed the two resonators at lower passband and a coupling structure is used to feed the two resonators at the upper passband. Two pairs of varactor-loaded resonators operating within two different frequency ranges, allow the independent passband frequency tuning. Using this configuration, it is convenient to tune the center frequency of each passband, while the responses of the other passband remain unaltered. Source-load coupling is realized to generate transmission zeros, resulting in high skirt-selectivity. The transmission zeros move synchronously with the passbands, ensuring sharp roll-off rate for all tuning states. To verify the proposed idea, a demonstration microstrip tunable bandpass filter is implemented. The simulated and measured results are presented.

1. INTRODUCTION

With the development of multi-band wireless communication, dual-band bandpass filter, as an important component in transceivers, has obtained great attention. In the past years, many design methods have been proposed. Among them, several methods are popularly used. The first method is to utilized two sets of resonators, one operates at the upper passband and the other at the lower passband [1–4]. By using this method, the frequencies and bandwidths can be

Received 29 May 2013, Accepted 9 July 2013, Scheduled 16 July 2013

* Corresponding author: Li Gao (gaoliscut@163.com).

independently controlled. However, the circuits occupy large area. For size reduction, stepped-impedance resonators (SIRs) are used to design dual-band filters [5–7]. By controlling the ratios of the electrical length and impedance of different part, the resonant frequencies of SIRs can be tuned. Unfortunately, the two frequencies are dependent, which complicate the design procedure. To facilitate the design method, stub-loaded resonators are proposed [8, 9]. It usually consists of a main transmission line and a stub. The resonant frequencies can individually be tuned by controlling the length of the main transmission line and stub. Besides the above methods, other structure such as defect ground structure [10] can also be used to design dual-band filters.

Recently, the stringent demand for low-cost reconfigurable communication systems such as cognitive radios requires the development of reconfigurable filters to cover a wide frequency range. In the past, tunable filters with single passband received much attention [11–24]. In [11, 12], bandpass filters with tunable center frequency were demonstrated. In [13], tunable bandpass filters with harmonic suppression were designed. Balanced tunable bandpass filters were also demonstrated [14]. In [15], another kind of tunable bandpass filter was presented, with the tuning of the passband bandwidth.

In comparison to single-passband tunable filters, there has been less work on dual-band tunable filters. In [22, 23], dual-band filters with non-tunable lower passband and tunable upper passband are reported. In [24], the two passbands can be tuned. However, the structure is complex which leads to a large circuit-board area and high insertion loss.

In this paper, we propose a compact dual-band filter with two independently-tunable passbands. The proposed filter consists of a novel feeding scheme and two pairs of varactor-loaded resonators. Each set of resonators generates one passband, resulting in dual-band responses. Two sets of bias voltages are applied to the varactors, enabling the independent passband tuning. Source-load coupling is realized to generate transmission zeros. Based on the proposed idea, a tunable dual-band filter is implemented. Both the simulated and measured results are presented.

2. DESIGN OF THE PROPOSED TUNABLE FILTER

There are two parts to demonstrate the design of the proposed tunable filter. Section 2.1 addresses the configuration of the filter. Section 2.2 focuses on the design procedure.

2.1. Filter Configuration

Figure 1(a) depicts the configuration of the proposed tunable dual-band microstrip bandpass filter. It consists of a feeding structure and two pairs of quarter-wavelength resonators. For each resonator, a varactor is loaded at the open end, as shown in Fig. 1(b). Capacitors C_1, C_2, C_3 and C_4 function as DC blocks. The topology of the proposed tunable dual-band filter is shown in Fig. 2. Resonators 1 and 2 are utilized to generate the lower passband. The voltage V_1 is applied to the varactor to change the electric length, allowing the tuning of the lower passband. A tap-coupled structure is utilized to feed the two resonators. At the lower passband frequency f_1, the short-ended microstrip lines, which are utilized to feed resonators 3 and 4,

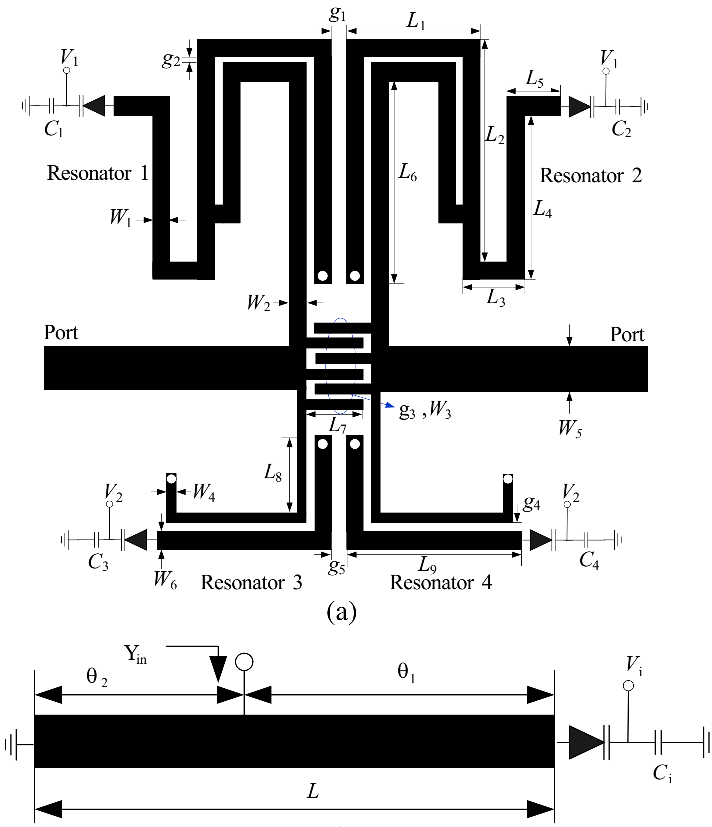

Figure 1. (a) Configuration of the proposed microstrip tunable filter. (b) The varactor- loaded resonator.

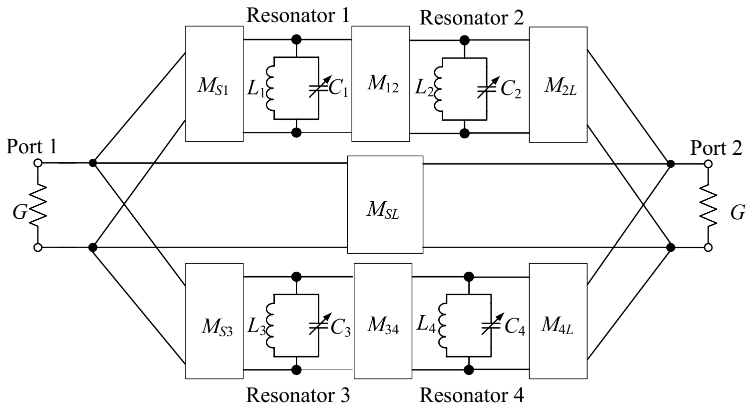

Figure 2. Filter topology.

function as loading elements of resonators 1 and 2 at f_1. Resonators 3 and 4 operate at the upper passband, with the bias voltage V_2. The two resonators are fed by short-ended transmission lines through the coupling structure. It is noted that two different feeding schemes for upper and lower passbands are used. This is because the coupling strength at the lower passband frequency is weaker than that at the upper frequency within the same coupling region. Therefore tap-coupling scheme is used to enhance the coupling strength at the lower passband. Source-load coupling is realized by the interdigital capacitor to generate transmission zeros. The interdigital coupling strength can be used to control the locations of the transmission zeros.

2.2. Design Procedure

In this work, a tunable dual-band filter is designed with the following specifications: The lower passband is tuned from 600 MHz to 700 MHz, with the passband fractional bandwidth (FBW) of around 7%. The upper passband is tuned from 1.2 GHz to 1.3 GHz, with the FBW of around 6%. The design procedure is as follows.

Step 1: The first step is to determine the resonator parameters and then get the desired passband frequencies. Fig. 1(b) shows the configuration of the varactor-loaded resonator. It consists of a short-ended microstrip line, a capacitor and a varactor. When the voltage is added to the varactor and the parasitic components of the varactor are ignored, it can equal to a capacitor C_v. By tuning the voltage, the capacitor will be changed, thus the resonant frequency can be tuned. The operating frequency is determined as follows. From Fig. 1(b), the input admittance Y_{in} can be expressed as follow:

$$Y_{in} = -j\frac{Yc}{\tan\theta 2} + Yc\frac{jb + jYc\tan\theta 1}{Yc + j(jb)\tan\theta 1} \quad (1)$$

where Y_c is the characteristics admittance, $b = \omega$C, and C corresponds to the combination of DC black capacitor C_i ($i = 1, 2, 3, 4$) and the varactor capacitance C_v. It is expressed as $C = C_iC_v/(C_i + C_v)$. From this, the resonant frequency can be deduced as follow:

$$f = \frac{\left[\arctan\left(\frac{Y_c}{b}\right) + n\pi\right] c}{2L\sqrt{\varepsilon_{eff}}} \quad (2)$$

where $n = 0, 1, 2, 3, \ldots, c$ is the speed of the light in free space, and ε_{eff} denotes the effective dielectric constant of the substrate.

For validation, the resonant frequencies are theoretically calculated using Matlab program based on Equation (2). It is assume that $C_i = 5\,\text{pF}$, $L = 20\,\text{mm}$, $\varepsilon_{eff} = 3.38$, $Y_c = 0.01\,\text{s}$, which fit the proposed filter design parameters. Also, the electromagnetic simulation using ADS is carried. The calculated and simulated results are shown in Fig. 3. It is seen that when the varactor capacitance is changed, the corresponding resonant frequencies can be altered. Moreover, the calculated results agree well with the simulated ones, demonstrating the effectiveness of Equation (2).

Step 2: The second step is to calculate the coupling matrix according to the required specifications and then determine the dimensions of the feeding and coupling structures.

The proposed filter uses two sets of resonators and thus the responses within the two passbands can be individually synthesized. It is noted that this is a tunable filter and thus there are numerous states, for instance, different frequencies and bandwidths. Herein, we select a typical set of design parameters within the scope of the required specifications and then calculate the coupling matrix [25].

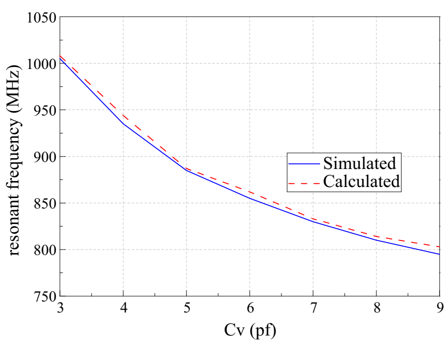

Figure 3. Calculated and simulated resonant frequencies.

For the lower passband, the typical parameters are selected to be: The center frequency is 600 MHz with bandwidth of 40 MHz, two transmission zeros located at 400 MHz and 800 MHz, respectively. Thus the coupling matrix is

$$M_{Lower} = \begin{bmatrix} 0 & 1.2881 & 0 & 0.0288 \\ 1.2881 & 0.1152 & -1.8404 & -0.0842 \\ 0 & -1.8404 & -0.0842 & 1.2828 \\ 0.0288 & -0.0842 & 1.2828 & 0 \end{bmatrix}$$

For the upper passband, the parameters are: The center frequency is 1300 MHz with bandwidth of 80 MHz, two transmission zeros located at 1080 MHz and 1450 MHz. Thus the coupling matrix is

$$M_{upper} = \begin{bmatrix} 0 & 1.2733 & 0 & 0.0758 \\ 1.2733 & 0.3567 & -1.7969 & -0.2467 \\ 0 & -1.7969 & -0.3599 & 1.2311 \\ 0.0758 & -0.2467 & 1.2311 & 0 \end{bmatrix}$$

Based on the above coupling matrix, the responses of lower and upper passban can be obtained as shown in the Figs. 4(a) and (b).

The above lower and upper passband responses are obtained individually due to the use of the two sets of resonators. To combine the two sets of resonators to obtain dual-band responses, a common feeding structure is utilized as shown in Fig. 1(a). Using this configuration, the external quality factors (Q_e) and the coupling coefficient (k) at the two passband can be individually controlled. At the lower passband, the tap-coupled structure is used to feed resonators 1 and 2. Thus, at the lower passband, Q_e is mainly determined by the gap g_2, the tap position and the line widths W_1 and W_2. The coupling between the resonators 1 and 2, k_{12}, is determined by the gap g_1 and corresponding coupling length. At the upper passband, Q_e is determined by the

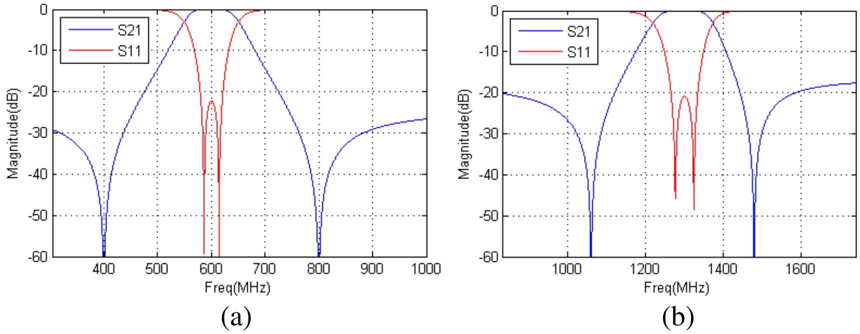

Figure 4. Calculated responses. (a) At lower passband, (b) at upper passband.

coupling strength between the short-ended feed lines and resonators, namely, g_4, L_8 and L_9. The coupling coefficient between resonators 3 and 4, k_{34}, is related to g_5 and associated coupling length. In this design, the Q_e and k at two specific passbands are independent because of the parallel feeding scheme. This provides a high degree of freedom to control the bandwidths of both passbands.

To obtain the desired Q_e and k, simulation is carried out to extract the parameters. Since this is a tunable filter, we choose a typical set of parameters which is the same as the one used in filter synthesis. In the process of extracting the Q_e and k for this tunable filter, the varactors are replaced by equivalent open-ended microstrip lines to realize the same desired responses. Then, the Q_e and k can be extracted using the following two formulas.

$$Q_e = \frac{f_0}{\Delta f_{\pm 90^\circ}} \tag{3}$$

$$k = \frac{f_2^2 - f_1^2}{f_2^2 + f_1^2} \tag{4}$$

where f_0 denotes the resonant frequency, $\Delta f_{\pm 90^\circ}$ the bandwidth about the resonant frequency over which the phase varies from -90 to 90 degree, and f_1 and f_2 are the higher and lower resonant frequencies, respectively. Based on the simulated results and this two equations, the Q_e and k are extracted as: $Q_{e1} = 11.45$, $k_{12} = 0.073$ for the lower passband, $Q_{e2} = 23.45$ $k_{34} = 0.12$ for the upper passband. This can satisfy the requirement and thus the coupling dimensions are determined. As for the source-load coupling strength M_{SL}, it will affect the responses of both lower and upper passbands. The desired M_{SL} at the lower and upper passbands are 0.0288 and 0.0758, respectively. The coupling strength can be adjusted by controlling the number of the coupling fingers, gap g_3, width W_3 and length L_7. However, the coupling strengths at the two passbands are controlled by the same inter-digital structure. Therefore, there is a trade-off between them to obtain acceptable performance at the two passbands.

Step 3: After the above two steps, the initial structure parameters can be obtained. Then, the varactors are added to the microstrip structure and the bias voltage is changed to obtain the frequency-tunable responses. Finally, fine tuning is performed to achieve good performance.

3. RESULTS AND DISCUSSION

To validate the proposed idea, a demonstration filter is fabricated on the substrate with a relative dielectric constant of 3.38, thickness of 0.81 mm and loss tangent of 0.0027. The filter configuration is shown in Fig. 1(a). The simulation and measurement results are accomplished by Zealand IE3D, ADS and Agilent's 5071C network analyzer, respectively. The design parameters are determined as Table 1. The values of capacities C_1, C_2, C_3, C_4 are 5 pF, 5 pF, 47 pF, and 47 pF, respectively. The varactors involved in the design are 1sv277 from Toshiba, with the tuning capacitance from 1 pF to 6 pF when the voltage is changed from 5 V to 0 V. The overall size of the filter is $0.067\lambda_g \times 0.040\lambda_g$, where λ_g is the guided wavelength at the lowest passband frequency. The photograph of the fabricated filter is shown in Fig. 5.

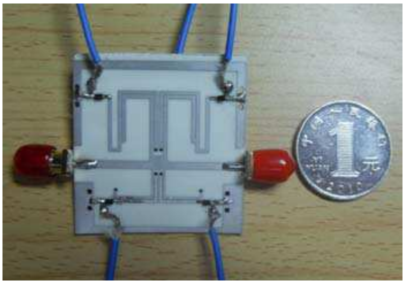

Figure 5. Photograph of the fabricated tunable filter.

Table 1. Dimensions (in millimeters) of the tunable filter.

Parameters	W_1	W_2	W_3	W_4	W_5	W_6	L_1	L_2	L_3	L_4
Value	0.8	0.9	0.4	0.4	1.84	0.8	9.5	13.8	3.1	12.7
Parameters	L_5	L_6	L_7	L_8	L_9	G_1	G_2	G_3	G_4	G_5
Value	2.8	12.5	2.0	6.0	11.0	0.4	0.2	0.2	0.2	0.4

Figures 6 and 7 depict the simulated and measured results, which show good agreement. The varactor model is the same as that in [15], except some components values are changed based on our previous experiments. The center frequency of the lower passband can be tuned within the range from 570 MHz to 700 MHz when the voltage V_1 varies from 1 V to 3.5 V. In this design, the frequency tuning range is mainly limited by the filter coupling and feeding scheme. When the voltage V_1 is tuned beyond this range, the passband responses become poor. The 3 dB bandwidth changes from 36 MHz to 60 MHz or 6.5% to 8.5%. The corresponding insertion loss is measured to be from 2.32 dB to 1.56 dB. The return loss within the passband is greater than 15 dB for all tuning states. The upper passband can be tuned from 1.156 GHz to 1.336 GHz when the voltage V_2 varies from 2 V to 4.8 V, with the

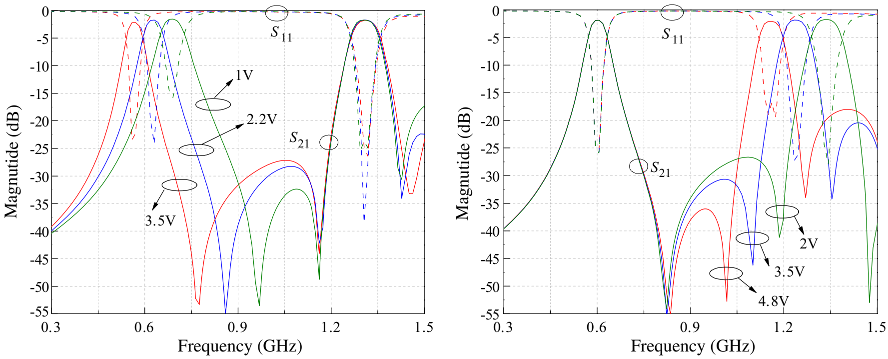

(a) (b)

Figure 6. Simulated responses. (a) Lower passband tuning, (b) upper passband tuning.

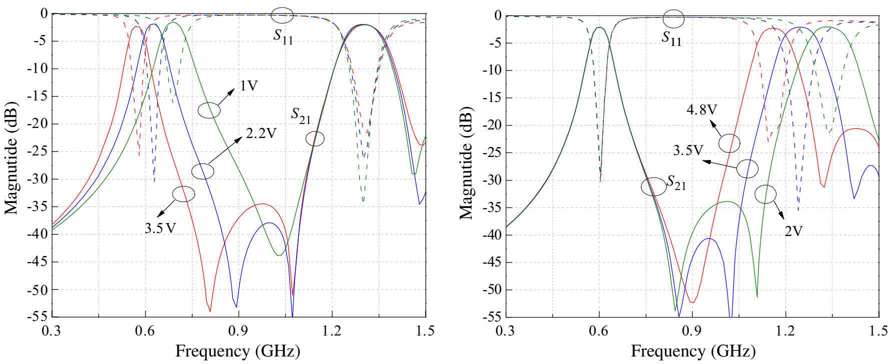

(a) (b)

Figure 7. Measured responses. (a) Lower passband tuning, (b) upper passband tuning.

bandwidth from 67 MHz to 85 MHz or 5.8% to 6.4%. The measured insertion loss is from 2.3 dB to 2.03 dB. The parasitic resistor of the varactor accounts for the insertion loss. When high-Q GaAs varactors or MEMS varactors are used, the loss can be reduced. The in-band return loss is greater than 15 dB for each tuning state. It is noted that changing the center frequency of one passband will not alter the responses of the other passband, featuring that the two passbands can be independently tuned. There are some discrepancies between the simulated and measured results. For instance, the measured bandwidth is wider than the simulated one. This is attributed to non-accuracy of the varactor model and fabrication errors. The input third-order intermodulation intercept point (IIP3) is 17 dBm at the two passbands with 1-MHz frequency spacing.

It is noted that there are three transmission zeros generated near the passband edges. They move together with the passbands, ensuring high selectivity for all tuning states. The transmission zeros are due to the source-load coupling. Theoretically, for both lower and upper passbands, the source-load coupling is available and four transmission zeros should be generated. However, it is difficult to obtain the desired the coupling strength for the lower and upper passbands in case of the tunable passbands. Therefore, there is a trade-off when determining the interdigital coupling strength. Accordingly, only three transmission zeros are observed in the simulation and measurement.

4. CONCLUSION

A high-selectivity tunable dual-band bandpass filter with independent passband tuning has been presented. A novel feeding scheme is utilized to combine two pairs of varactor-loaded quarter-wavelength resonators. Changing the operating frequency of one passband does not alter the performance of the other one, enabling the independent passband tuning. Source-load coupling is utilized to generate transmission zeros which move together with the passbands and ensure high selectivity for each tuning state. Both simulation and experiment show that the two passbands can be independently tuned with good performance.

ACKNOWLEDGMENT

The work was supported by the NSFC under 61001055 61271060 and U1035002, the NCET under NCET-10-0402.

REFERENCES

1. Chen, Z.-X., X.-W. Dai, and C.-H. Liang, "Novel dual-mode dual-band bandpass filter using double square-loop structure," *Progress In Electromagnetics Research*, Vol. 77, 409–416, 2007.
2. Liu, H., L Y. Zhao, L. Shi, and H. Luo, "Dual-band bandpass filter design using open-loop resonators," *Microw. Opt. Tech. Lett.*, Vol. 54, 2370–2371, 2012.
3. Chen, C. F, T. Y. Huang, and R. B. Wu, "Design of dual- and triple-passband filters using alternately cascaded multiband resonators," *IEEE Trans. on Microw. Theory and Tech.*, Vol. 54, No. 9, 3550–3558, 2006.

4. Chen, Y. and C. Y. Hsu, "A simple and effective method for microstrip dual-band filters design," *IEEE Microw. Wireless Compon. Lett.*, Vol. 16, 246–248, 2006.
5. Weng, M. H., C. H. Kao, and Y. C. Chang, "A compact dual-band bandpass filter with high band selectivity using cross-coupled asymmetric SIRs for WLANs," *Journal of Electromagnetic Waves and Applications*, Vol. 24, Nos. 2–3, 161–168, 2010.
6. Ma, D., Z. Y. Xiao, L. Xiang, X. Wu, C. Huang, and X. Kou, "Compact dual-band bandpass filter using folded SIR with two stubs for WLAN," *Progress In Electromagnetics Research*, Vol. 117, 357–364, 2011.
7. Ha, J., S. Lee, B.-W. Min, and Y. Lee, "Application of stepped-impedance technique for bandwidth control of dual-band filters," *IEEE Trans. on Microw. Theory and Tech.*, Vol. 60, No. 7, 2106–2114, 2012.
8. Zhang, X. Y., J.-X. Chen, Q. Xue, and S.-M. Li, "Dual-band bandpass filters using stub-loaded resonator," *IEEE Microw. Wireless Compon. Lett.*, Vol. 17, No. 8, 583–585, 2007.
9. Xu, K.-D., Y.-H. Zhang, C.-L. Zhuge, and Y. Fan, "Miniaturized dual-band bandpass filter using short stub-loaded dual-mode resonators," *Journal of Electromagnetic Waves and Applications*, Vol. 25, No. 16, 2264–2273, 2011.
10. Wu, G.-L., W. Wu, X.-W. Dai, and Y.-C. Jiao, "Design of novel dual-band bandpass filter with microstrip meander-loop resonator and CSRR DGS," *Progress In Electromagnetics Research*, Vol. 78, 17–24, 2008.
11. Long, J., C. Z. Li, W. Z. Cui, J. T. Huangfu, and L. X. Ran, "A tunable microstrip bandpass filter with two independently adjustable transmission zeros," *IEEE Microw. Wireless Compon. Lett.*, Vol. 21, No. 2, 74–76, 2011.
12. Sekar, V., M. Armendariz, and K. Entesari, "A 1.2–1.6 GHz substrate-integrated-waveguide RF MEMS tunable filter," *IEEE Trans. on Microw. Theory and Tech.*, Vol. 59, No. 4, 866–876, 2011.
13. Zhang, X. Y., Q. Xue, C. H. Chan, and B.-J. Hu, "Low-loss frequency-agile bandpass filters with controllable bandwidth and suppressed second harmonic," *IEEE Trans. on Microw. Theory and Tech.*, Vol. 58, No. 6, 1557–1564, 2010.
14. Li, Y. C. and Q. Xue, "Tunable balanced bandpass filter with constant bandwidth and high common-mode suppression," *IEEE Trans. on Microw. Theory and Tech.*, Vol. 59, No. 10, 2452–2460, 2011.

15. Miller, A. and J.-S. Hong, "Wideband bandpass filter with reconfigurable bandwidth," *IEEE Microw. Wireless Compon. Lett.*, Vol. 20, No. 1, 28–30, 2010.
16. Chen, J.-X., J. Shi, Z.-H. Bao, and Q. Xue, "Tunable and switchable bandpass filters using slot-line resonators," *Progress In Electromagnetics Research*, Vol. 111, 25–41, 2011.
17. Saha, S. C., U. Hanke, H. Sagberg, T. A. Fjeldly, and T. Saeher, "Tunable band-pass filter using RF MEMS capacitance and transmission line," *Progress In Electromagnetics Research C*, Vol. 23, 233–247, 2011.
18. Wang, S. and R.-X. Wang, "A tunable bandpass filter using Q-enhanced and semi-passive inductors at S-band in 0.18-μm CMOS," *Progress In Electromagnetics Research B*, Vol. 28, 55–73, 2011.
19. Gharbi, R., H. Zairi, T. Hichem, and H. Baudrand, "Tunable lowpass filters using folded slots etched in the ground plane," *Progress In Electromagnetics Research C*, Vol. 7, 65–78, 2009.
20. Moghimi, M. J., H. Ghafoori-Fard, and A. Rostami, "Multi-wavelengths optical switching and tunable filters using dynamic superimposed photorefractive Bragg grating," *Progress In Electromagnetics Research C*, Vol. 3, 129–142, 2008.
21. Sun, J. S., N. Kaneda, Y. Baeyens, T. Itoh, and Y.-K. Chen, "Multilayer planar tunable filter with very wide tuning bandwidth," *IEEE Trans. on Microw. Theory and Tech.*, Vol. 59, No. 11, 2864–2871, 2011.
22. Zhang, X. Y. and Q. Xue, "Novel centrally loaded resonators and their applications to bandpass filters," *IEEE Trans. on Microw. Theory and Tech.*, Vol. 56, No. 4, 913–921, 2008.
23. Dirbau, D., A. Lázaro, A. Pérez, E. Martinez, L. Pradell, and R. Villarino, "Tunable dual-band resonators for communication systems," *International Journal of Microwave and Wireless Technologies*, Vol. 2, 245–253, 2010.
24. Djournessi, E. E., M. Chaker, and K. Wu, "Varactor-tuned quarter-wavelength dual-bandpass filter," *IET Microw. Antennas & Propagation*, Vol. 3, No. 1, 117–124, 2009.
25. Amari, S., "Direct synthesis of folded symmetric resonator filters with source-load coupling," *IEEE Microw. Wireless Compon. Lett.*, Vol. 11, No. 6, 264–266, 2001.